True amplitude DMO, offset continuation and AVA/AVO for curved reflectors

Sergey Fomel, Stanford Exploration Project, Stanford University; Norman Bleistein, Herman Jaramillo, and Jack K. Cohen Center for Wave Phenomena, Colorado School of Mines*

Summary

We describe asymptotic analysis of true amplitude DMO processing and of an offset continuation partial differential equation. They are equivalent at offset zero in 2.5D. However, the OC result is true for all offsets and does not depend on the 2.5D assumption. We further show how the output of the DMO processing can be used for AVO/AVA analysis.

Introduction

Dip moveout (DMO) maps data at finite offset to *pseudo zero-offset* data. Offset continuation (OC) maps common-offset data from one offset to another. Thus, DMO is a special case of offset continuation with final offset, zero. In this paper, we describe analysis of the amplitude of DMO and OC for the response to curved reflectors in a constant background medium.

DMO maps the arrival times of reflection "events" at zero-offset arrival times. However, analysis of the effect on amplitude has, until now, been incomplete; earlier work Liner [1990, 1991], Bleistein [1990], Black, et al. [1993], Zhang [1988], described the amplitude mapping of DMO on model data for planar reflectors. However, analysis of curvature effects was lacking. We present that here. (See, Tygel, etal, 1995a,b for an alternative approach to this problem.)

Offset continuation provides another approach to the DMO problem and is more general [Fomel, 1995a, 1995b; Deregowski and Rocca, 1981; Bolondi, etal., 1982]. This method is based on a kinematically derived wave equation in offset, midpoint, and time [Fomel, 1994, Goldin and Fomel, 1995]. Thus, it properly predicts the transformation of traveltime, since it is derived from the kinematics of OC. This approach was also shown to predict the same DMO amplitude result presented here for the curved reflector response in 2.5D. However, the amplitude analysis of OC for mapping to arbitrary offset has not been carried out before. The derivation of the OC partial differential equation—OCPDE—is based on kinematics alone—essentially, a differential equation for wave propagation predicted from a dispersion relation, equivalent to proposing the wave equation from knowledge of the eikonal equation, alone. This approach cannot guarantee that the amplitude is correct; only the second order terms of the OCPDE are predictable from the kinematics. This method misses first order terms in the OCPDE these are terms that would effect amplitude. We confirm by the analysis described here that, for the leading order "WKBJ" amplitude, there are no such "missing" first order terms in the OCPDE earlier [Fomel, 1994, Goldin and Fomel, 1995].

Below is a list of the results of our analysis of amplitude for DMO and OC.

(i) The input offset traveltime is mapped to the zero-offset traveltime by the DMO processing and it is mapped to the output offset traveltime by the OC partial differential equation.

(ii) The reflection coefficient at the input offset is preserved; neither formalism maps the initial reflection coefficient to a new "final" value.

(iii) For DMO, the bandwidth of the source is scaled by the cosine of the incidence angle and the source signature in the frequency domain is compressed into a smaller bandwidth. For OC, the bandwidth is scaled by the ratio of cosines of incidence angles; the bandwidth is compressed when mapping to smaller offsets and stretched when mapping to larger offsets.

(iv) The input offset geometrical spreading that characterizes the dip of the reflector, alone, is mapped to the corresponding zero-offset geometrical spreading by DMO or to the output offset geometrical spreading factor by the OCPDE.

(v) The new result here is that the input offset geometrical spreading due to reflector curvature is mapped to the output offset geometrical spreading effect due to curvature. This is true for either the DMO or for the solution of the OCPDE. For DMO, this new result has been proven only for the *two-and-one-half dimensional*—2.5D—case. For OC, the result is not restricted to 2.5D.

For AVO/AVA analysis, we propose two DMO processing formulas whose ratio on reflection event peaks is the cosine of the specular incidence angle at the input nonzero-offset. Thus, for a given event on the zero-offset trace, the ratio of these outputs at variable offsets, $2h$, provides us data for a table of specular incidence angles, $\theta_S(h)$. We propose, here, a method for stripping away all constituents of amplitude except the reflection coefficient. This leads to an estimate of the angularly dependent reflection as a function of h and allows us to add a third column to our table, $R(\cos\theta_S(h))$, to complete the data set for AVO/AVA analysis.

The DMO formalism

To derive of the true amplitude DMO formalism, we use Born inversion for common-offset data cascaded with

Born modeling to zero-offset to produce a zero-offset data set from the input finite offset data set—both for a constant background speed, c. The common-offset is $2h$ around a variable midpoint, y.

Symbolically, $u(y,\omega,h)$ to $u_0(x_0,\omega_0)$:

$$u_0(x_0,\omega_0) = \mathcal{M}\Big[\mathcal{I}_h\left[u(y,\omega,h)\right]\Big]. \tag{1}$$

The inner operator $\mathcal{I}_h$ produces a Born approximate Earth model, $\alpha_h(\xi_1,\xi_3)$, while the outer operator $\mathcal{M}$ produces zero-offset data from this Earth model. The cascaded kernel is a function of $y,\omega,h,\xi_1,\xi_3,x_0,\omega_0$ with integrations over y,ω,ξ_1,ξ_3, while *the input data only depends on the variables,* y,ω,h. Thus, we apply stationary phase to carry out the integrals in ξ_1,ξ_3, thereby reducing the processing in (1) to integration over the variables, y,ω, that appear in the data.

This formalism is a mapping from space/frequency to space/frequency, easiest for asymptotic analysis. However, we can transform this operator to the more familiar variables of Hale DMO by using asymptotics, again. The result is

$$u_0(x_0,\omega_0) = \frac{1}{2\pi}\int \frac{dk dt_n}{A}\left[1+\frac{2k^2h^2}{\omega_0^2 t_n^2}\right] \cdot U(k,t,h)\exp\{i\Theta\}, \tag{2}$$

$$t_n = \sqrt{t^2-(2h/c)^2}, \quad A = \sqrt{1+(kh/\omega_0 t_n)^2},$$

$$\Theta = kx_0 + \omega_0 t_n A.$$

The result (2) differs from Hale's through the factor in square braces under the integral sign.

The Born approximation yields point scatterer modeling. Thus, we have no *a priori* idea of how this operator will treat reflection data. To determine these effects, we apply the formula to ray theoretic or Kirchhoff-approximate reflection data and use asymptotic analysis to carry out all of the necessary integrations. It is this output that leads to the interpretations described in the next section.

DMO results

Here, we explain our DMO result with simple WKBJ or ray theoretic models for the response to an arbitrary curved reflector in 2.5D. In Figure 1, the zero-offset point x_0 and the finite offset source/receiver pair, $y\mp h$, share the same specular point, $(x(s),z(s))$. For a single anticlinal specular point,* as shown in the figure, the finite offset reflection data is given asymptotically by

* The analysis is valid for synclinal reflection points, including buried foci.

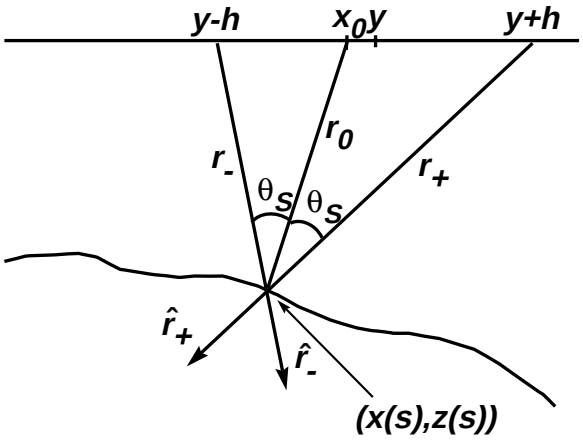

Figure 1. Specular geometry for DMO processing.

$$u(y,\omega,h) = \frac{F(\omega)R(\cos\theta_S)}{4\pi(r_+ + r_-)}\sqrt{\frac{\rho_0\cos^2\theta_S}{r_0+\rho_0\cos^2\theta_S}} \cdot \exp\{i\omega(r_+ + r_-)/c\}, \tag{3}$$

with zero-offset limiting form,

$$u(x_0,\omega,0) = \frac{F(\omega)R(1)}{8\pi r_0}\sqrt{\frac{\rho_0}{r_0+\rho_0}} \cdot \exp\{2i\omega r_0/c\}. \tag{4}$$

Here, $F(\omega)$ is the source signature and $R(\cos\theta_S)$ is the geometrical optics reflection coefficient at specular incidence angle θ_S; $R(1) = R(\cos 0)$ is the zero offset (normal incidence) reflection coefficient. For finite offset, the traveltime from source to reflector to receiver at propagation speed c is $(r_+ + r_-)/c$; for zero-offset, the traveltime is $2r_0/c$. The factor, $1/(r_+ + r_-)$ is the planar geometrical spreading depending on the dip of the reflector, only, while the factor,

$$\sqrt{\frac{\rho_0\cos^2\theta_S}{r_0+\rho_0\cos^2\theta_S}},$$

is the spreading effect due to curvature; ρ_0 is the radius of curvature at the specular point. The geometrical dip spreading effect for the zero-offset model is $2r_0$. Note that the effect of curvature at any offset is expressed in terms of r_0, and that it differs from the zero-offset curvature effect only in that the *effective* radius of curvature is $\rho_0\cos^2\theta_S$ in the finite offset case.

By asymptotic analysis, we find that the output of our DMO processing on reflection data is

$$u_0(x_0,\omega_0) = \frac{F(\omega_0\sec\theta_S)R(\cos\theta_S)}{8\pi r_0}\sqrt{\frac{\rho_0}{r_0+\rho_0}} \cdot \exp\{2i\omega r_0/c\}. \tag{5}$$

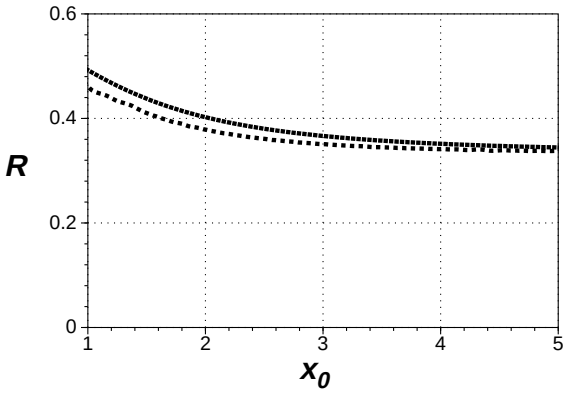

Figure 2. Theoretical and computed reflection coefficient for a circular reflector.

A comparison of equations (3), (4) and (5) will confirm the list of features of the DMO processing outlined above.

A numerical check on this claim is provided by the following example. We generate synthetic data for reflection from a circular cylinder and process it with our DMO formalism. We estimate the effects of geometrical spreading and source signature to examine the reflection coefficient from the DMO output position after DMO and compare to the known result for this geometry. In Figure 2, we show both results, with the theoretical result shown in black and the output of the DMO formalism shown in gray. The parameters used were $2h$ = 1km; depth of the top of the circular reflector, 1km; radius of the reflector, 1km; frequency range, 25-100Hz; velocity above the reflector, 2km/s, velocity below the reflector, 4km/s. The theoretical and computed values of the finite offset reflection coefficient are seen to be in good agreement over the range of zero-offset points, 1km-5km, with the maximum error at the left end, less than 5%.

Offset continuation

The OCPDE derived in earlier papers [Fomel, 1994, 1995a] is

$$h\left(\frac{\partial^2 P}{\partial y^2}-\frac{\partial^2 P}{\partial h^2}\right)=t_n\,\frac{\partial^2 P}{\partial t_n\,\partial h}\,. \tag{6}$$

We solve this equation by the WKBJ method in the time domain. This leads to the following eikonal and transport equations for the traveltime and amplitude of P:

$$h\left[\left(\frac{\partial \tau_n}{\partial y}\right)^2-\left(\frac{\partial \tau_n}{\partial h}\right)^2\right]=-\,\tau_n\,\frac{\partial \tau_n}{\partial h}\,, \tag{7}$$

and

$$\left(\tau_n-2h\,\frac{\partial \tau_n}{\partial h}\right)\,\frac{\partial A_n}{\partial h}+2h\frac{\partial \tau_n}{\partial y}\frac{\partial A_n}{\partial y}$$
$$+hA_n\left(\frac{\partial^2 \tau_n}{\partial y^2}-\frac{\partial^2 \tau_n}{\partial h^2}\right)\;=\;0\,. \tag{8}$$

Let us consider Kirchhoff approximation model data for reflection in 3D:

$$u_S(y+h,y-h,t)=\int_\Sigma R(y+h,y-h,\mathbf{x}(\sigma))\mathbf{d}\sigma$$
$$\cdot\frac{\partial}{\partial n}\left[A_s(\mathbf{x}(\sigma),y-h)\;A_r(\mathbf{x}(\sigma),y+h)\right. \tag{9}$$
$$\left.\cdot\;f\left(t-\tau_s[\mathbf{x}(\sigma),y-h]-\tau_r[\mathbf{x}(\sigma),y+h]\right)\right].$$

One can show that the integrand on the second and third lines here satisfies the eikonal equation and transport equation (7) and (8). This means that if we hold R at its value for the input offset, the remainder of the amplitude propagates in accordance with the OCPDE, (6), to the order of accuracy of WKBJ. However, we know that the application of the method of stationary phase to this Kirchhoff data with fixed R will exactly produce the right geometrical spreading—both planar and 3D curvature effects—for any offset h. In particular, if we propagate the solution of the OCPDE to $h=0$ and specialize to 2.5D, it will produce the result (4), above. These are the results we claimed in the Introduction.

AVA/AVO analysis

We consider now the result (5) in the time domain, for fixed value of x_0, focusing on a particular reflection event, and evaluate the output at its peak value; that is, when the time variable, $t_0=2r_0/c$. The peak value is given by

$$U_0\mathrm{PEAK}=\cos\theta_S\,\frac{R(\cos\theta_S)}{4r_0}\sqrt{\frac{\rho_0}{r_0+\rho_0}}F_0,$$
$$F_0=\frac{1}{2\pi}\int F(\omega)d\omega. \tag{10}$$

We now introduce a second DMO operator,,

$$u_1(x_0,\omega_0)=\frac{1}{2\pi}\int\frac{dktdt_n}{t_nA^2}\left[1+\frac{2k^2h^2}{\omega_0^2t_n^2}\right]$$
$$\cdot\,U(k,t,h)\exp\{i\omega_0\Theta\}, \tag{11}$$

which differs from the operator (2) only in the multiplier, $t/(t_nA)$. The same asymptotic analysis that produced our peak prediction, (10), also predicts that

$$U_1\mathrm{PEAK}=\frac{R(\cos\theta_S)}{4r_0}\sqrt{\frac{\rho_0}{r_0+\rho_0}}F_0. \tag{12}$$

Now we have the tools for AVA/AVO analysis. First, *the ratio of the two peak outputs provides an estimate of* $\cos\theta_S$ *for each value of* h! Thus, we obtain

a table of values of $\cos\theta_S$ as a function of h simple by graphing the ratio, $U_0\text{PEAK}/U_1\text{PEAK} = \cos\theta_S$, as a function of h. Second, for constant background, the arrival time of this event produces an estimate of geometrical spreading in both peak outputs. To proceed further, we require data at critical reflection. We recognize the critical offset by a cusp in the graph of the peak amplitude versus offset. At this critical offset, we can estimate $\cos\theta_S$ again, now for $\theta_S = \theta_{\text{critical}}$, but we also know that $R = 1$ at critical. So, the only unknown in (12) at critical is the product,

$$\sqrt{\frac{\rho_0}{r_0+\rho_0}}F_0,$$

and we determine that product from the critical angle output! This factor is a constant of the outputs for all offsets, hence we can divide it out of our output, $U_1\text{PEAK}$, leaving us with an estimate of R for each choice of h or $\cos\theta_S$.

Of course, we do not know the spatial location of this reflection even, but only where it resides in time on the trace at x_0, for all h. To find its spatial location, it would be necessary to actually carry out the zero-offset migration on the DMO transformed (and stacked) pseudo zero-offset data.

This is the AVA/AVO analysis for true amplitude DMO processing.

Conclusions

We have described here results of asymptotic analysis of a true amplitude DMO processing algorithm and of an offset continuation partial differential equation. They are equivalent at offset zero in 2.5D. However, the OC result is true for all offsets and does not depend on the 2.5D assumption. It is thereby a far more general result. We have further shown how the output of the DMO processing could be used for a limited AVO/AVA analysis. The limitations are, first, that we only know the trace location of the reflection even, not its spatial location and, second, that we require observations at sufficient wide offset to observe critical reflection.

Acknowledgement

The authors thank the ACTI/LANL Project, Center for Wave Phenomena Consortium Project at the Colorado School of Mines and the Stanford Exploration Project at Stanford University. The second author also gratefully acknowledges the support and encouragement of Fabio Rocca on the analysis of the OCPDE.

References

Black, J. L., Schleicher, K. L., and Zhang, L., 1993, True amplitude imaging and dip moveout: Geophysics, 58, 1, 47-66.

Bleistein, N., 1984, "Mathematical Methods for Wave Phenomena," Academic Press Inc. (Harcourt Brace Jovanovich Publishers), New York.

Bleistein, N., 1990, Born DMO revisited: 60th Annual International Meeting of the Society of Exploration Geophysicists, Expanded Abstracts, 1366-1369.

Bolondi G., E. Loinger and F.Rocca, 1982, Offset continuation of seismic sections, Geophys. Prosp., 30, 6, 813-828.

Deregowski S. M., and F. Rocca, 1981, Geometrical optics and wave theory of constant offset sections in layered media: Geophys. Prosp., 29, 3, 374-406.

S. B. Fomel, 1994, Kinematically equivalent differential operator for offset continuation of reflected wave seismograms: Russian Geology and Geophysics, 35, 9, 122-134.

Fomel, S., 1995a, Amplitude preserving offset continuation in theory, Part 1: the offset continuation equation: Stanford Exploration Project preprint, SEP-84, 179-196.

Fomel, S., 1995b, Amplitude preserving offset continuation in theory, Part 2: solving the equation: Stanford Exploration Project preprint, SEP-89.

S. V. Goldin and S. B. Fomel, 1995, Estimation of reflection coefficient in DMO: Russian Geology and Geophysics, 36, 4, 103-115.

Hale, I. D., 1984, Dip-moveout by Fourier transform: Geophysics, 49, 6, 741-757.

Liner, C. L., 1990, General theory and comparative anatomy of dip moveout: Geophysics, 55, 5, 595-607.

Liner, C. L., 1991, Born theory of wave-equation dip moveout: Geophysics, 56, 2, 182-189.

Sullivan, M. F., and Cohen, J. K., 1987, Pre-stack Kirchhoff inversion of common offset data, Geophysics, 52, 745-754.

Tygel, M., Schleicher, J., and Hubral, P., 1995a, Dualities between reflectors and reflection time surfaces: Journal of Seismic Exploration, Vol. 4, pp. 123 - 150.

Tygel, M., Schleicher, J., and Hubral, P., 1995b, True-amplitude migration to zero offset (MZO) by diffraction stack: preprint Insitituto de Matemática Estatística e Ciência da Computação, Universidade Estadadual de Campinas, Brazil.

Zhang, L., 1988, A new Jacobian for dip-moveout: Stanford Exploration Project, SEP-59, 201-208.